Contents

Regular papers

The 18-electron principle can be explained by invoking s and d bonding contributions at the metal M, combined with the nodal structure of the ligand system, L_n. No metal p orbitals are necessarily required.
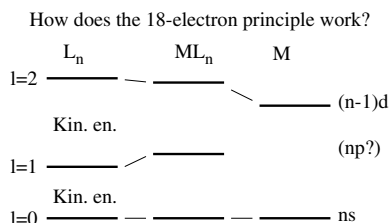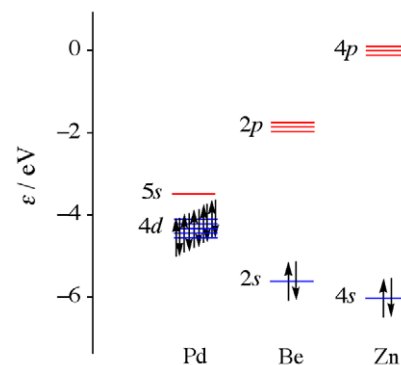
The transition metal Pd is intrinsically more reactive towards oxidative insertion into a C–X bond than alkaline earths and group-12 transition metals. This can be mainly ascribed to palladium's excellent electron-donating and accepting capabilities associated with the high-energy 4d HOMO and low-energy 5s LUMO.
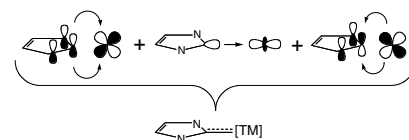
Based on DFT calculations the NHC–[TM] bond is analyzed in terms of σ-donation, π-backdonation and π-donation contributions.
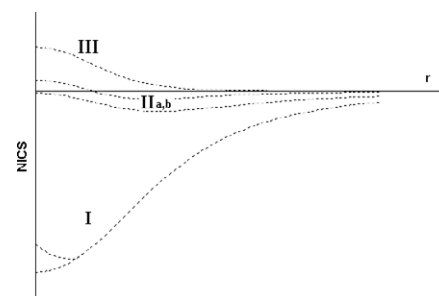
Contents

A series of rare-earth metal alkyl complexes $[Ln(\eta^5-C_5Me_4ZNR'-\kappa N)(CH_2SiMe_3)(THF)_n]$ (Ln = Y, Lu; Z = SiMe$_2$, CH$_2$SiMe$_2$; R′ = tBu, Ph, C$_6$H$_4$-tBu-4, C$_6$H$_4$-nBu-4) was examined for catalytic activity in the hydrosilylation of 1-decene and styrene under standard conditions using PhSiH$_3$. A significant influence of the ligand structure on the catalytic property (turnover frequency, regioselectivity) was observed.
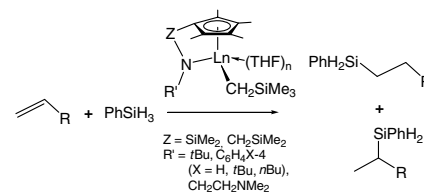
The mechanism of hydrosilylation with the model complex $[Cp(H_3P)Ru(H)_2Si(H)Ph]^+$ and possible alternative pathways are investigated with quantum chemical methods. The analysis of the electron density distribution of the catalytic active complex shows surprising bond features between Ru and Si. It is necessary to make drastic changes in the ligand environment of the transition metal–silicone complex to observe cycloaddition reactions.
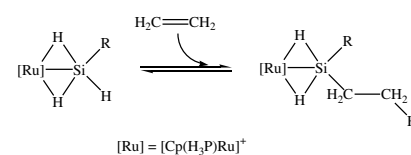
A theoretical study of the molecular structure of complex $[RuCl\{C_6H_3(CH_2P(C_6H_5)_2)_2-2,6\}(PPh_3)]$ ($[RuCl(PCP^H)(PPh_3)]$, **1**) and its tetrakis-pentafluorophenyl substituted analogue $[RuCl\{C_6H_3-(CH_2P(C_6F_5)_2)_2-2,6\}(PPh_3)]$ ($[RuCl(PCP^{F20})(PPh_3)]$, **2**) has been carried out to rationalise the observed structural changes observed in **2** compared to **1** upon replacement of C$_6$H$_5$- by C$_6$F$_5$-groups. The results of the calculations, performed on the models $[(C_6F_5PH_2)_2Cl]^-$ and $[(C_6H_5PH_2)_2Cl]^-$, show that in complex **2** the chloride ligand interacts with the axial fluorinated phenyl rings. The spectroscopic features of both complexes have been interpreted with the TD-DFT method.
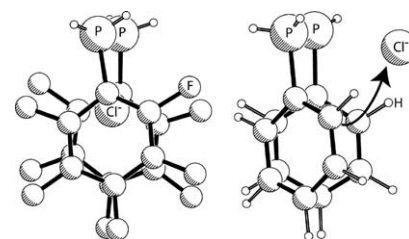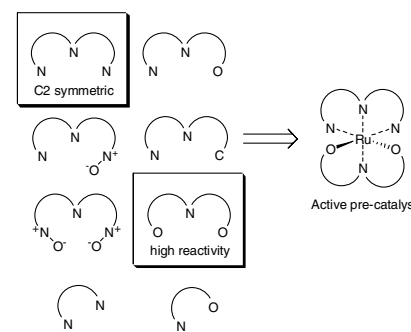
Possible active intermediates of the ruthenium-catalyzed epoxidation of olefins using H$_2$O$_2$ are proposed based on synthetic, spectral, catalytic activity and computational studies of ruthenium bipyridine and terpyridine complexes. This fragment based analysis of the catalytic system suggests also reasons for low catalytic activity and low enantiomeric induction of some catalysts. A simple catalytic system utilizing UHP has also been developed in which all six classes of aromatic olefins can be epoxidized in moderate to good yields with good chemoselectivity.
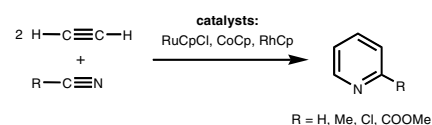
The mechanism of the catalytic formation of
pyridines from the coupling of two alkynes
and the nitriles $N \equiv CR$ (R = H, Me, Cl,
COOMe) with the fragments CpRuCl, CpCo,
and CpRh has been investigated by means of
DFT/B3LYP calculations.

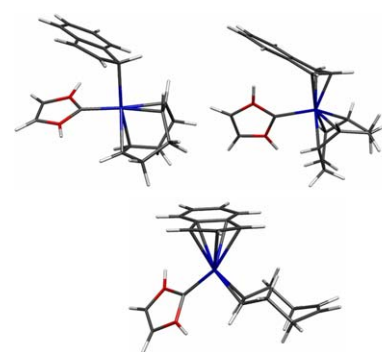Although both $[Ir(\eta^4\text{-COD})(NHC^{Cy})(\eta^1\text{-Cp})]$
and $[Ir(\eta^2\text{-COD})(NHC^{Me})(\eta^5\text{-Cp})]$ have been
characterized as derivatives of the $Ir(\eta^4\text{-}$
$COD)(NHC^R)$ fragment, the only indenyl
complex isolated for this system was $[Ir(\eta^4\text{-}$
$COD)(NHC^R)(\eta^1\text{-Ind})]$. DFT calculations
showed that the energies of η^1-Ind, η^3-Ind,
and η^5-Ind complexes are close enough to be
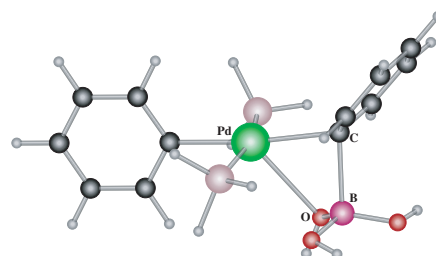consistent with a fluxional behavior in solu-
tion.

DFT calculations confirm that the palladium-
catalyzed Suzuki–Miyaura cross-coupling be-
tween phenyl bromide and phenylboronic acid
requires the presence of a base, and suggest
that the mechanism starts with the attack of
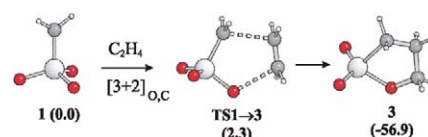the base on the organoboronic acid.

Quantum chemical calculations of the reaction
profile for addition of ethylene to $OsO_3(CH_2)$
show that there are several reactions pathways
besides the most favorable $[3+2]_{O,C}$ addition.

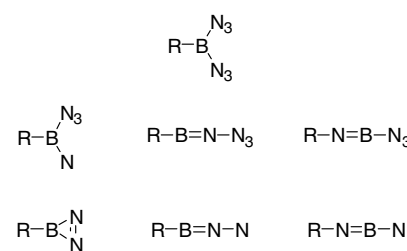The copper(II) catalyzed Michael reaction of enamines derived from 1,3-diketones and amino acids most likely involves as a key intermediate an aza-enolate coordinated to three sites of a square planar copper centre.
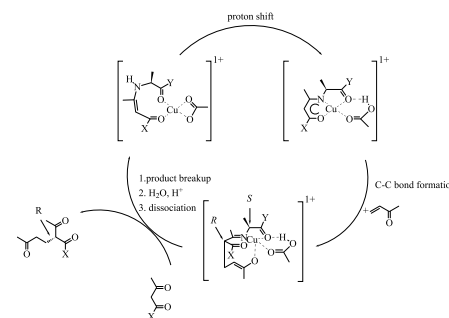
Energies and structures of $PhBN_6$, $PhBN_4$, and $PhBN_2$ isomers are investigated computationally.

Density functional theory (DFT) has been employed to investigate the rate-determining step for the Shilov reaction in which $PtCl_4^{2-}$ can catalyze H–D exchange of alkanes in acidic aqueous solution. C–H activation and methane uptake are the two possible candidates.
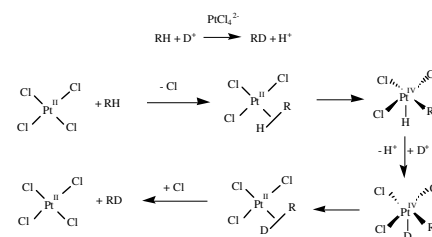
The computational study of the carbonylation of allyl substrates catalyzed by nickel and palladium, shows interesting mechanistic features. In particular, irrespective of the metal used in the catalysis, the favored path is very similar in the two cases (i.e., a direct attack of the halogen on the metal).
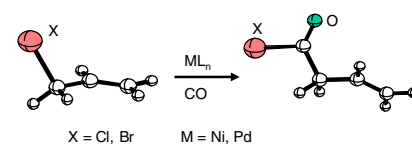
In Pd-catalyzed allylic substitutions, the sensitivity for electronic differentiation is higher for earlier transition structures, due to closer Pd–C_α contacts. This even overcompensates smaller intrinsic differentiation with *para*-nitro pyridine ligands, which yields the highest *cis* vs. *trans* differentiation and selectivity.
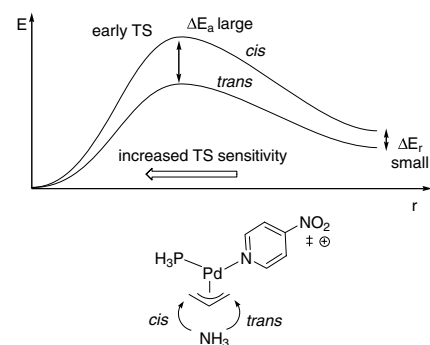
Heteronuclear metal complexes such as [Cl(CO)$_2$(dppe)W≡C(–C$_6$H$_4$–C≡C)$_p$–C$_6$H$_4$–N≡C–]$_2$PdI$_2$ (p = 0–3) have been prepared. The electronic interaction between the remote metal centers has been probed by a variety of spectroscopic techniques.
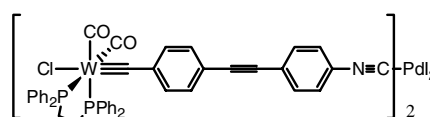
Density functional theory calculations are used to predict the structure and the ionization energies of some analogues of iron-only hydrogenases.
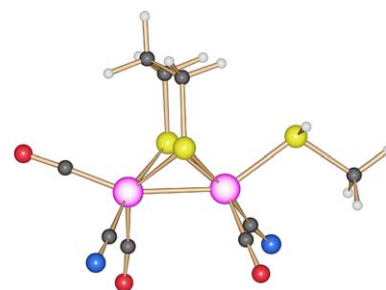
Six titanium pentafulvene complexes are theoretically investigated and indicate a gradual change of the fulvene ligand coordination to the titanium center for dianionic η^5,η^1- to olefinic η^6-coordination. Time-dependant DFT calculations reproduce the experimental UV data reasonably well. The absorption maxima correspond to a ligand-to-metal charge transfer from the HOMO to the LUMO+1 of the complexes.
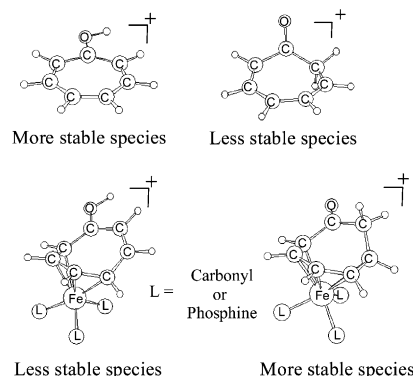
More stable species   Less stable species

Less stable species   More stable species

(M = Fe: **1**; Ru: **2**)   (M = Fe: **1′**; Ru: **2′**)

(**5′**-H)$^-$